AD-A169 137 PARTIALLY CAVITATING FLOWS ABOUT FOILS(U) DAVID W TAYLOR NAVAL SHIP RESEARCH AND DEVELOPMENT CENTER BETHESDA MD C C HSU MAR 86 DTNSRDC-86/014 1/1

UNCLASSIFIED F/G 13/10 NL

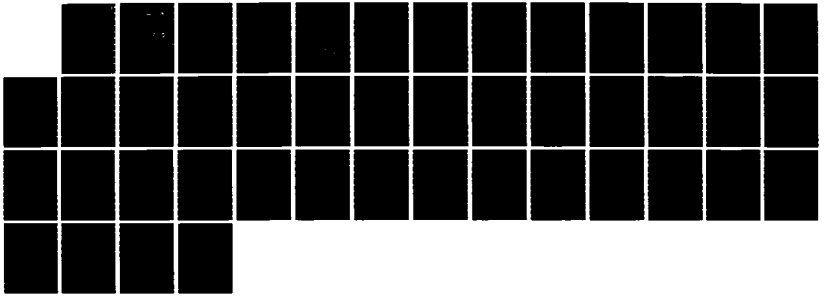

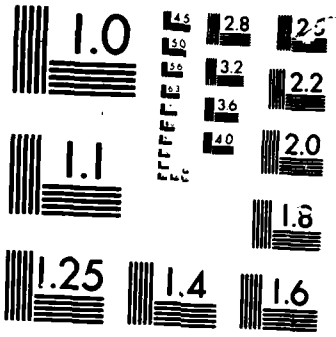

MICROCOPY CHART

AD-A169 137

PARTIALLY CAVITATING FLOWS ABOUT FOILS

by

C.C. Hsu

DTIC
ELECTE
S JUL 2 1986 D
B

APPROVED FOR PUBLIC RELEASE; DISTRIBUTION IS UNLIMITED.

DTIC FILE COPY

SHIP PERFORMANCE DEPARTMENT
RESEARCH AND DEVELOPMENT REPORT

March 1986

DTNSRDC-86/014

86 7 1 239

UNCLASSIFIED
SECURITY CLASSIFICATION OF THIS PAGE

REPORT DOCUMENTATION PAGE

1a REPORT SECURITY CLASSIFICATION UNCLASSIFIED	1b RESTRICTIVE MARKINGS
2a SECURITY CLASSIFICATION AUTHORITY	3 DISTRIBUTION / AVAILABILITY OF REPORT APPROVED FOR PUBLIC RELEASE; DISTRIBUTION IS UNLIMITED.
2b DECLASSIFICATION / DOWNGRADING SCHEDULE	
4 PERFORMING ORGANIZATION REPORT NUMBER(S) DTNSRDC-86/014	5 MONITORING ORGANIZATION REPORT NUMBER(S)
6a NAME OF PERFORMING ORGANIZATION David W. Taylor Naval Ship R&D Center 6b OFFICE SYMBOL (If applicable) Code 1522	7a NAME OF MONITORING ORGANIZATION David W. Taylor Naval Ship R&D Center Code 1504
6c ADDRESS (City, State, and ZIP Code) Bethesda, Maryland 20084-5000	7b ADDRESS (City, State, and ZIP Code) Bethesda, Maryland 20084-5000
8a NAME OF FUNDING / SPONSORING ORGANIZATION Naval Sea Systems Command 8b OFFICE SYMBOL (If applicable) SEA 05R24	9 PROCUREMENT INSTRUMENT IDENTIFICATION NUMBER
8c ADDRESS (City, State, and ZIP Code) Washington, D.C. 20360	10 SOURCE OF FUNDING NUMBERS PROGRAM ELEMENT NO: 61153N PROJECT NO: SR02301 TASK NO: SR0230101 WORK UNIT ACCESSION NO: DN505001

11 TITLE (Include Security Classification)
PARTIALLY CAVITATING FLOWS ABOUT FOILS

12 PERSONAL AUTHOR(S)
Hsu, C.C.

13a TYPE OF REPORT	13b TIME COVERED	14 DATE OF REPORT (Year, Month, Day)	15 PAGE COUNT
Final	FROM TO	1986, March	43

16 SUPPLEMENTARY NOTATION

17 COSATI CODES			18 SUBJECT TERMS (Continue on reverse if necessary and identify by block number)
FIELD	GROUP	SUB-GROUP	Partially cavitating flows, foils, cavity length, cavity volume.
20	04		

19 ABSTRACT (Continue on reverse if necessary and identify by block number)

A practical approach for predicting partially cavitating flow characteristics of foil sections is presented. The method takes into account indirectly the viscous flow effects and the interaction between the fully wetted and perturbed cavitating flows. The partially cavitating flow characteristics are found to be sensitive to variations in the angle of attack, camber, thickness, and the thickness distribution. Some comparisons between the calculated and measured cavity lengths are made, and the results are generally in good agreement. Further developments needed in the future are also discussed.

20 DISTRIBUTION / AVAILABILITY OF ABSTRACT	21 ABSTRACT SECURITY CLASSIFICATION
☒ UNCLASSIFIED/UNLIMITED ☐ SAME AS RPT ☐ DTIC USERS	UNCLASSIFIED
22a NAME OF RESPONSIBLE INDIVIDUAL C.C. Hsu	22b TELEPHONE (Include Area Code) (202) 227-1611 22c OFFICE SYMBOL Code 1522

DD FORM 1473, 84 MAR — 83 APR edition may be used until exhausted. All other editions are obsolete.

SECURITY CLASSIFICATION OF THIS PAGE
UNCLASSIFIED

TABLE OF CONTENTS

LIST OF FIGURES

Accession For
NTIS
DTIC
Unannounced
Justification
By
Distribution/
Availability Codes
Dist | Avail and/or Special
A-1

DTIC ELECTE JUL 2 1986 S D B

QUALITY INSPECTED 3

NOTATION

a	Parameter related to NACA camber mean line
a_1	Parameter related to cavity length
b_1	Parameter related to cavity detachment point
$C_{L\alpha,m}$	Measured fully wetted flow lift slope
c	Chord length
c_o, c_1	Constants in formula for complex potential
c_{ℓ_1}	Design lift coefficient
D	Total drag
D_o	Drag due to fully wetted flow
D_1	Drag due to cavitation
Im	Denotes imaginary part of
L	Total lift
L_o	Lift due to fully wetted flow
L_1	Lift due to cavitation
ℓ	Cavity length
q_o	Local flow speed due to fully wetted flow
q_1	Local flow speed due to cavitation
q_c	Cavity speed
q_o^*	Fully wetted velocity at the position of minimum pressure
Re	Denotes real part of

U	Free Stream speed
u, v	Velocity component in x, y coordinates
$\bar{V}$	Cavity volume
x,y	Horizontal and vertical ordinates in physical plane
x_d	Chordwise position of cavity detachment
x_m	Chordwise position of fully wetted pressure minimum
z	Complex variable, $x + iy$
α	Angle of attack
δ	Cavity wake thickness
ζ	Complex variable, $\xi + i\eta$
ξ,η	Horizontal and vertical ordinates in transformed ζ-plane
θ_o	Local fully wetted flow angle
θ_1	Local flow angle due to cavitation
ρ	Fluid density
σ	Cavitation number
Γ	Circulation
Γ_{ideal}	Ideal-flow circulation
ϕ	Total scalar potential
ϕ_o	Scalar potential due to fully wetted flow
ϕ_1	Scalar potential due to cavitation
ψ	Complex potential, $\phi + i\psi$

ψ	Stream function
Ψ'	Complex velocity
Ψ_0'	Complex velocity due to fully wetted flow
Ψ_1'	Complex velocity due to cavitation
ω	Hodograph variable, ln Ψ'
ω_o	Hodograph variable, ln Ψ_0' due to fully wetted flow
ω_1	Hodograph variable, ln Ψ_1' due to cavitation

ABSTRACT

A practical approach for predicting partially cavitating flow characteristics of foil sections is presented. The method takes into account indirectly the viscous flow effects and the interaction between the fully wetted and perturbed cavitating flows. The partially cavitating flow characteristics are found to be sensitive to variations in the angle of attack, camber, thickness, and the thickness distribution. Some comparisons between the calculated and measured cavity lengths are made, and the results are generally in good agreement. Further developments needed in the future are also discussed.

ADMINISTRATIVE INFORMATION

The work reported herein was supported by the General Hydromechanics Research Program under Task Area SR0230101 and Work Unit 1522-025.

INTRODUCTION

There is concern with avoiding problems and reducing the likelihood of propeller-induced hull vibration, noise, and blade erosion on Navy ships. The unsteady surface pressure excitation and local flow instability responsible for these problems are associated with blade sheet cavity geometry and cavity dynamics. Reliable computational tools for the analysis of propeller blade sheet cavitation would be useful for assessments of given propeller/wake/hull arrangements and for guidance of new propeller geometries intended to keep blade cavitation and excitation levels under some control.

Realistic estimates of hull surface pressure excitation produced by unsteady cavity volume variation depend on accurate definition of cavity geometry. Tulin and Hsu[1,2*] have observed, for instance, that predictions of partially cavitating flows about a lifting surface are very much influenced by the surface velocity distributions calculated for fully wetted flows about the foil sections and by the conditions used for the cavity closure. Linearized theories for lifting foils all predict an infinite suction-pressure peak at the foil leading edge, with an inverse square root singular behavior. This propagates difficulties into the analysis of the cavitating flow over the foil, especially for the cavity geometry. Linear cavity flow theories show inaccurate cavity predictions for

*References are listed on page 11.

the location of the sheet cavity leading edge, the sensitivity of the cavity extent and cavity thickness to changes in the foil thickness, and foil angle of attack. It has also been shown[2] that details of the cavity-closure condition can affect the overall hysteresis-like behavior of unsteady leading edge cavitation.

Examples of linearized analysis of two-dimensional, partially cavitating flows about lifting foils and some applications of the results to three-dimensional propeller blade problems are found in References 3 through 9. Generally, the results of the complete propeller analysis schemes are fairly good in that the principle features of the steady and unsteady blade cavitation and propeller performance are at least represented in the predictions.

There are, however, persistent difficulties with the cavitating flow aspects of the available calculation schemes, leading to a degree of unreliability in the predictions. As an example, consider the Massachusetts Institute of Technology unsteady cavitating propeller analysis program developed by Lee,[6] and known by the acronym PUF-3. When applied to high speed ships (~30 knots) the usual prediction for blade cavitation from this computation scheme typically shows excessive cavity length over the outer blade region, compared with observations.

Recently, a nonlinear numerical method for the analysis of two-dimensional, partially cavitating lifting foils has been developed by Uhlman[10] based on the distribution of line-vortex elements on the boundaries of the foil and cavity. This important work has been useful in (a) illustrating the differences in trends between the linear and nonlinear predictions for crucial cavity flow features, and (b) showing qualitative agreement with the existing results of Tulin and Hsu. Unfortunately, the method requires very large computation time and cost, involving large numbers of boundary elements and many iterations to arrive at very slowly converging solutions. It does not appear that such a large computational effort can be tolerated at the present time inside a large-scale three-dimensional calculation scheme for an entire propeller.

An important building block for the eventual realistic analysis of complete propeller blade flow is a reliable yet (fast running) efficient computer program for the prediction of partial chord length cavitation and the hydrodynamic loads developed on two-dimensional foil sections operating in high speed steady and unsteady inflow conditions. The present work describes results for an approach that holds great promise for both accuracy and calculation speed.

With the fully wetted flow assumed known, a partially cavitating flow theory was developed by Tulin and Hsu.[1] This theory offers the following advantages: (a) it deals with the effect of leading edge radius; (b) it can be applied as a two-dimensional perturbation to a known three-dimensional flow. Some salient features of Tulin-Hsu theory are outlined.

In the original treatment of Tulin and Hsu, the cavity is assumed to be detached from the leading edge, and the circulation of the fully wetted flow is taken to be the ideal-flow value. Both of these assumptions are not generally realized in practice. The theory of Tulin-Hsu is modified here to account for some of the real flow effects, and is used to predict the cavitation performance of various NACA (National Advisory Committee for Aeronautics) sections. Some comparisons between the calculated and measured cavity lengths are made, and the results are found to be generally in good agreement. Further developments needed in the future are also discussed.

OUTLINE OF TULIN-HSU THEORY

Consider two-dimensional inviscid flows with small regions of cavitation and define:

$$\Psi = (\phi/U) + i(\psi/U) \quad \text{(the complex potential)} \tag{1}$$

$$d\Psi/dz = \Psi' = \Psi_0'\Psi_1' = (u/U) - i(v/U) \quad \text{(the complex velocity)} \tag{2}$$

$$\Psi_0' = q_0 e^{-i\theta_0} \quad \text{(no cavitation)} \tag{3}$$

$$\Psi_1' = q_1 e^{-i\theta_1} \tag{4}$$

represents the effect of cavitation, so that

$$\Psi_1' = 1 \tag{5}$$

if no cavitation occurs. The flow in the physical and complex potential plane is shown in Figure 1. The problem, as posed, utilizes the single spiral vortex model for cavity termination.

For the solution, it is useful to define the function:

$$\omega = \omega_0 + \omega_1 = \ln q_0 - i\theta_0 + \ln q_1 - i\theta_1 \tag{6}$$

The ω_o, representing the contribution from the fully-wetted flow, is assumed to be known. The problem is then reduced to that of finding ω_1 with the boundary conditions:

$$\mathrm{Re}(\omega_1) = \ln q_1 = \ln (q_c/q_0) \qquad \phi_B<\phi<\phi_D \tag{7}$$

where $q_c = \sqrt{1+\sigma}$ (σ = cavitation number) and

$$\mathrm{Im}(\omega_1) = 0 \qquad \begin{cases} \phi_A<\phi<\phi_B & \\ & \psi = 0^+ \\ \phi_D<\phi<\phi_E & \\ & \\ \phi_A<\phi<\phi_E & \psi = 0^- \end{cases} \tag{8}$$

The conditions at infinity are:

$$\mathrm{Re}(\omega_1) = 0 \tag{9}$$

$$\mathrm{Im}(\omega_1) = 0 \tag{10}$$

The approximate cavity closure condition is:

$$\mathrm{Im} \oint \omega_1 d\Psi = (D_1/\rho U^2) = \delta_c \tag{11}$$

where D_1 is the cavity drag.

The problem as formulated may be greatly simplified with the aid of t conformal transformation:

$$\zeta = -ia_1\sqrt{\frac{(\Psi/\phi_E)}{(\Psi/\phi_E)-1}} = \xi + i\eta \tag{12}$$

or

$$\Psi/\phi_E = \zeta^2/(\zeta^2+a_1^2) \tag{13}$$

where

$$a_1 = \sqrt{(\phi_E/\phi_D)-1} \tag{14}$$

which maps the complex potential plane onto the ζ-half plane as shown in Figure 2.

The associated boundary conditions, conditions at infinity, and the closure condition are given respectively by:

$$\mathrm{Re}(\omega_1) = \ln(q_c/q_0) \qquad -1<\xi<-b_1 \tag{15}$$

$$\mathrm{Im}(\omega_1) = 0 \qquad -\infty<\xi<-1 \tag{16}$$

$$\mathrm{Re}\left(\omega_1(-ia_1)\right) = 0 \tag{17}$$

$$\mathrm{Im}\left(\omega_1(-ia_1)\right) = 0 \tag{18}$$

$$\mathrm{Im}\oint \omega_1(d\Phi/d\zeta)d\zeta = (D_1/\ell^2) = \tau_c \tag{19}$$

The appropriate solution of the mixed boundary value problem is then given by:

$$\omega_1 = -\frac{\sqrt{\zeta+b_1}}{\zeta\sqrt{\zeta+1}}\left\{\frac{i}{\pi}\int_{-1}^{-b_1}\frac{\bar{\zeta}\sqrt{\bar{\zeta}+1}\left[\ln\sqrt{1+\sigma}-\ln q_0\right]}{\sqrt{\bar{\zeta}+b_1}(\zeta-\bar{\zeta})}\,d\bar{\zeta}+c_0+c_1\zeta\right. \tag{20}$$

The value of a_1 is assumed specified, which is equivalent in specifying the cavity length. The constants c_o, c_1, and σ are determined from Equations (17), (18), and (19). Note that D_1 in Equation (19) is not known a priori; a satisfactory solution can, however, be obtained in two or three iterations.

For a first approximation, the lift and drag due to cavitation may be expressed as:

$$L_1 + D_1 = -\rho U^2 \oint \omega_1 (d\Psi/d\zeta)\,d\zeta \tag{21}$$

and the cavity volume is given by:

$$\bar{V} = -\mathrm{Im}\oint \omega_1 \Psi (d\Psi/d\zeta)\,d\zeta \tag{22}$$

SOME PRACTICAL APPLICATIONS

The cavitating flow perturbation ω_1, as seen in Equation (20), depends only upon the local fully wetted velocity distribution, q_o, and cavity detachment point. In the original treatment of Tulin and Hsu, the cavity is assumed to detach from the leading edge ($b_1 = 0$), and the fully wetted velocity distribution is assumed to be determined by perfect fluid theory; such assumptions may not be realized in practice.

The velocity distribution is generally modified by the viscous boundary layer and wake. The effect of viscous wake on the circulation defect, according to Spence and Beasley,[11] may be approximated by:

$$\Gamma = (\mathrm{LIFT}/\rho U) = \Gamma_{\mathrm{ideal}}\left[1-0.214\sqrt{(D/0.5\rho U^2 c)}\right. \tag{23}$$

where $D = D_o + D_1$ = total drag and c = chord length. The boundary layer effect on circulation depends on shapes and transition positions of foils and is quite cumbersome to estimate. In the present application, measured lift-curve slopes will be used for estimating fully wetted velocity distributions. For a first approximation, Equation (23) is also utilized to account for some of the interactions between the fully wetted and the perturbed cavitating flows.

Cavitation inception at high speeds generally occurs at the position of minimum pressure. In the present approach, the cavity is assumed to detach at the point where the fully wetted pressure is minimum. The exact location of detachment is, of course, also dependent on fluid properties, ambient flow conditions, and transition positions. Such influences can be substantial in laboratory studies when test Reynolds numbers are low.

In the following, the partially cavitating flow characteristics of various NACA sections are analyzed. For such sections, ideal-flow values of the fully wetted velocity distributions are tabulated in Appendices I and II of Reference 12. In the first iteration, the value of D_1 is taken to be zero. For the subsequent iterations, the value of D_1 is approximated by:

$$D_1 = L_0\alpha\left[1-\left(\sigma/q_0^{*2}\right)\right] \tag{24}$$

where L_o = fully wetted lift, q_o^* = fully wetted velocity at the position of minimum pressure, and α = angle of attack. Wind tunnel measured values of lift curve slope at chord Reynolds number = 6×10^6 (presented in Figure 57 of Reference 12) are used to correct the ideal fully wetted velocity distributions. Although the calculated results can only be applied strictly to the cases in which the chord Reynolds numbers are close to 6×10^6; such results are believed to be approximately valid for higher Reynolds numbers (up to about 10^8); the correction due to the variation of Reynolds number in the ranges of $10^7 \sim 10^8$ is probably not significant. Extensive numerical calculations have been made; however, only selective results of salient interest are presented here.

In Figures 3 and 4, the variations of cavity length and volume with angles of attack and cavitation numbers for NACA 66-006 section are shown. The length and volume of the cavity, for a given α/σ, generally increase with increasing angle of attack. The cavity length and cavity volume for cambered NACA

66-006 with a = 1.0 meanline, and $\alpha = 4^o$ are given in Figures 5 and 6. The effect of increasing design camber is to increase the length and volume of the cavity. Some of the partially cavitating flow characteristics for NACA 66-006, NACA 66-008, NACA 66-010, and NACA 66_1-012 sections are shown in Figures 7 and 8. The length and volume of the cavity, in general, decrease rapidly with increasing foil thickness. The partially cavitating flow characteristics are also found to depend on thickness distributions. Shown in Figures 9 and 10 are some calculated results for NACA 66-006, NACA 63-006, and NACA 0006 sections with $\alpha = 4^o$. The NACA 0006 section, which has leading edge radius = 0.004c produces smaller cavity lengths and cavity volumes than those produced by the NACA 63-006 and NACA 66-006 sections for $\alpha/\sigma < 0.05$; but for $\alpha/\sigma > 0.05$, the NACA 0006 section produces larger cavity lengths and cavity volumes than those of NACA 63-006 and NACA 66-006 sections. The leading edge radii of NACA 63-006 and NACA 66-006 are 0.00297c and 0.00223c, respectively.

Some comparisons between the calculated and the measured cavity lengths are shown in Figures 11 through 14. The foils for which systematic experimental observations are available include: NACA 4412 (Kermeen),[13] NACA 66_1-012 (Kermeen),[14] 10.5% Joukowsky section (Shen and Peterson),[15] NACA 64A006 (McCullough and Gault).[16] In analyzing NACA 4412, NACA 66_1-012, and NACA 64A006 sections, measured lift curve slopes for the fully wetted flow are used for the first iteration. For the Joukowsky section, the value of 2π for lift-curve slope is used for the calculations. The data of McCullough and Gault are wind tunnel measurements for leading edge separation, the cavitation numbers and cavity lengths are inferred from pressure coefficient measurements (from Figure 3 of Reference 16). The agreement between theory and measurements is in general good. The results lend credence to both the present theoretical development and method of calculation.

DISCUSSION

The partially cavitating flow characteristics of hydrofoil sections are found to be sensitive to variations of angle of attack, camber, thickness and thickness distribution.

Foil section thickness has an important influence. For a given α/σ, the cavity extent (length) generally decreases with increasing thickness ratio,

as seen in Figure 7. The effect of thickness distribution and leading edge radius is somewhat more complicated. In Figure 9, with a comparison at the same thickness ratio, the NACA 00xx sections (with larger leading edge radius than NACA 6-series sections) produce shorter cavities for small values of α/σ <0.05. For larger values of α/σ, NACA 6-series sections generally produce the shorter cavities. About the same trend holds for the sectional cavity volume. Thus, depending on the operating ranges of α/σ, the choice of foil section for the least amount of partial cavitation can vary considerably.

The theory presented herein takes into account the proper pressure distribution at the leading edge of the noncavitating foil flow. It is substantially different from that in the linearized theories. Some comparisons between results of the present calculations and results of linear theory are displayed in Figure 15 for NACA 16-series sections. In these calculations, the value of 2π is used for the lift curve slope. It is seen that the linear theory provides substantial misrepresentation of the effect of section thickness on cavity extent. Linear theory predicts an increase in cavity length with increasing thickness ratio, contrary to the correct trend predicted by the present analysis.

By using measured values of lift-curve slope for fully wetted flow, the present results also take into account indirectly some of the viscous flow effects. Example variations of computed cavity lengths associated with changes in lift curve slopes for NACA 66-006 section are given in Figure 16, and are seen to be substantial. Lift reduction due to viscosity depends on foil trailing edge angles and may not be small, especially for chord Reynolds number $<10^6$. In these cases, the viscous-flow effects on the partially cavitating flow characteristics can become very important.

The present theory also accounts for some of the reduction in circulation due to the effect of cavity wake. This is accomplished by using Equations (23) and (24). The interaction effect involves a reduction of foil lift that is caused by the flow retardation associated with the cavity drag. It can be substantial if the cavity drag is large. In Figure 17, the magnitude of this influence is indicated as the variation of cavity length for the NACA 66-006 section with and without the interaction effect included.

Flow characteristics of partially cavitating foils vary also with the positions of cavity detachment and cavity closure conditions. Variations of

cavity length with different detachment points are given, for example, in Figure 18 for the NACA 66-006 section at $\alpha = 4^o$ incidence. This compares the results for detachment at the leading edge ($x_d = 0$) with those using the minimum pressure point ($x_d = x_m$) for fully wetted flow. In the present example the value of x_m ($\simeq 0.00026$) is quite small. Values of x_m are much larger for thicker sections with smaller angles of attack, and the effect of cavity detachment positions on the partially cavitating flows can be substantial. In Figure 19, the predicted cavity length variations due to different closure conditions for NACA 66-006 section are displayed, and are shown to be significant. Since the cavity closure condition may vary rapidly in unsteady flows, it can have a very important effect on time-varying properties of partially cavitating flows.

CONCLUSIONS AND RECOMMENDATIONS

The present approach permits an efficient and fast-running solution to the partially cavitating flow problem to be carried out in terms of a known fully wetted flow velocity distribution. This analysis can be readily applied to unsteady flows if the time rate of change is not too rapid. The perturbed cavitating flow can thus be analyzed at any given time based upon the instantaneous values of angle of attack. A similar approach may also be applied to unsteady three-dimensional flows if the fully wetted flow does not vary too rapidly in the spanwise direction.

Further work should be carried out along several lines to exploit the present successful analysis of partially cavitating realistic-foil sections. (1) The steady results should be extended to include unsteady inflow variations of arbitrary frequency in order to cover cases of rapid-time variability. (2) With the two-dimensional analysis complete for steady and unsteady cases, the results should be applied to make a comprehensive study on the influence of section shape on performance features of partially cavitating foils. New foil shapes will be generated that have certain desirable features for use as propeller blade sections. Examples of sought-after properties might include: the best lift-to-drag performance for given cavity length and/or volume; the least cavity length and volume for given foil lift; and the least inherent unstable cavity behavior under typical unsteady conditions. (3) The present nonlinear sectional flow analysis approach should be incorporated into a global lifting-surface analysis scheme for unsteady propeller performance.

REFERENCES

1. Tulin, M.P. and C.C. Hsu, "The Theory of Leading Cavitation on Lifting Surfaces with Thickness," Proceedings of Symposium on Hydrodynamics of Ship and Offshore Propulsion Systems, Oslo, Norway (1977).

2. Tulin, M.P. and C.C. Hsu, "New Applications of Cavity Flow Theory," 13th Symposium on Naval Hydrodynamics, Tokyo, Japan (1980).

3. Acosta, A.J., "A Note on Partial Cavitation of Flat Plate Hydrofoil," California Institute of Technology Hydrodynamics Laboratory Report No. E-19.9 (1955).

4. Geurst, J.A., "Linearized Theory for Partially Cavitated Hydrofoils," International Shipbuilding Progress, Vol. 6, No. 60 (1959).

5. Noordzij, L., "Pressure Field Induced by a Cavitating Propeller," International Shipbuilding Progress, Vol. 23, No. 260 (1976).

6. Lee, C.S., "Prediction of the Transient Cavitation on Marine Propellers by Numerical Lifting-Surface Theory," 13th Symposium on Naval Hydrodynamics, Tokyo, Japan (1980).

7. Hoshino, T., "Estimation of Unsteady Cavitation on Propeller Blades as a Base for Predicting Propeller-Induced Pressure Fluctuations," Journal of the Society of Naval Architects of Japan, Vol. 148 (1980).

8. Isshiki, H. and M. Murakami, "On a Theoretical Treatment of Unsteady Cavitation (3rd Report)," Transactions of West-Japan Society of Naval Architects No. 64 (1982).

9. Van Houten, R.J., "The Numerical Prediction of Unsteady Sheet Cavitation on High Aspect Ratio Hydrofoils," 14th Symposium on Naval Hydrodynamics, Ann Arbor (1982).

10. Uhlman, J.S., "The Surface Singularity Method Applied to Partially Cavitating Hydrofoils," Ph.D. Thesis, Massachusetts Institute of Technology, Department of Ocean Engineering (1983).

11. Spence, D.A. and J.A. Beasley, "The Calculation of Lift Slopes, Allowing for Boundary Layer, with Applications to the RAE 101 and 104 Aerofoils," Aeronautical Reserch Council Reports and Memoranda No. 3137 (1958).

12. Abbott, I.H. and A.E. Von Doenhoff, "Theory of Wing Sections," Dover Publications, Inc., New York (1958).

13. Kermeen, R.W., "Water Tunnel Tests of NACA 4412 and Walchner Profile 7 Hydrofoils in Noncavitating and Cavitating Flows," California Institute of Technology Engineering Report No. 47-5 (1956).

14. Kermeen, R.W., "Water Tunnel Tests of NACA 66_1-012 Hydrofoils in Noncavitating and Cavitating Flows," California Institute of Technology Engineering Report No. 47-7 (1956).

15. Shen, Y.T. and F.B. Peterson, "Unsteady Cavitation on an Oscillating Hydrofoil," 12th Symposium on Naval Hydrodynamics, Washington, D.C. (1978).

16. McCullough, G.B. and D.E. Gault, "Boundary-Layer and Stalling Characteristics of the NACA 64A006 Airfoil Section," National Advisory Council for Aeronautics Technical Note No. 1923 (1949).

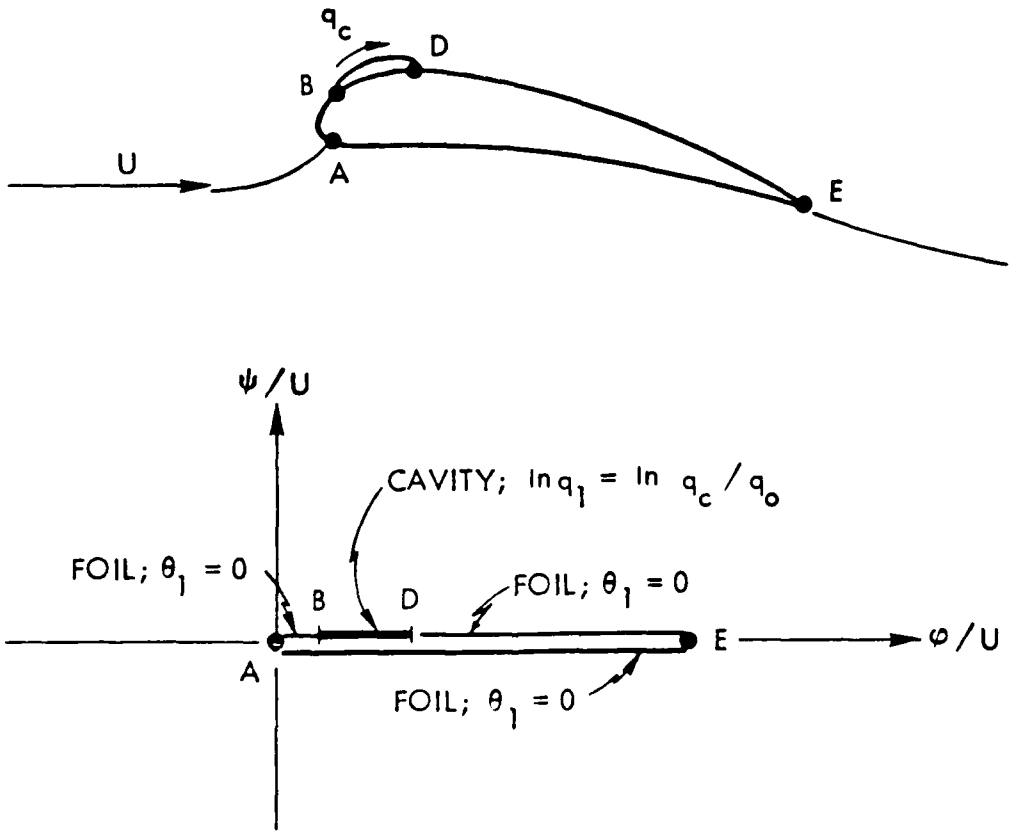

Figure 1 - Schematics of Partially Cavitating Flow and Boundary Value Problems

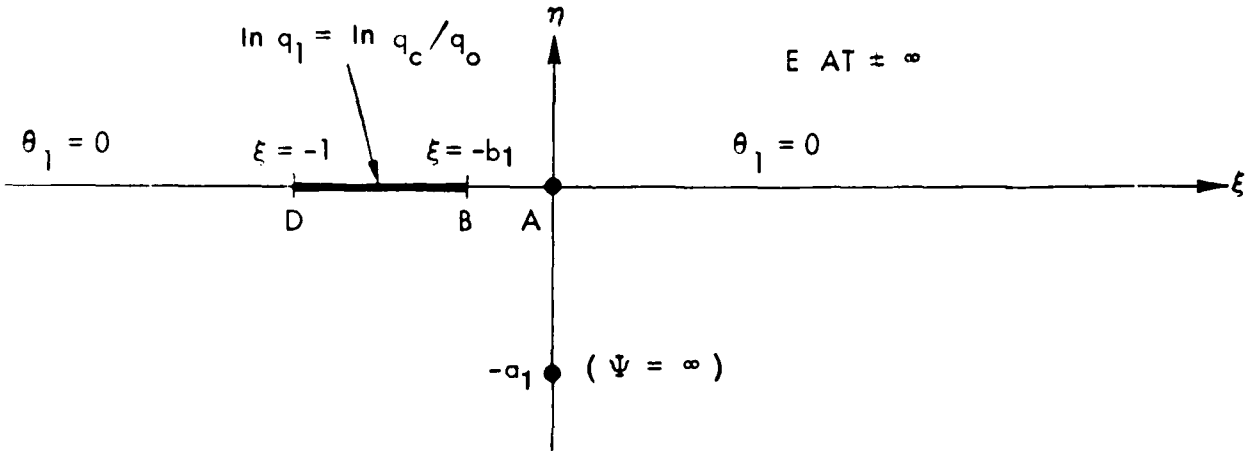

Figure 2 - Boundary Value Problems in Transformed ζ-Plane

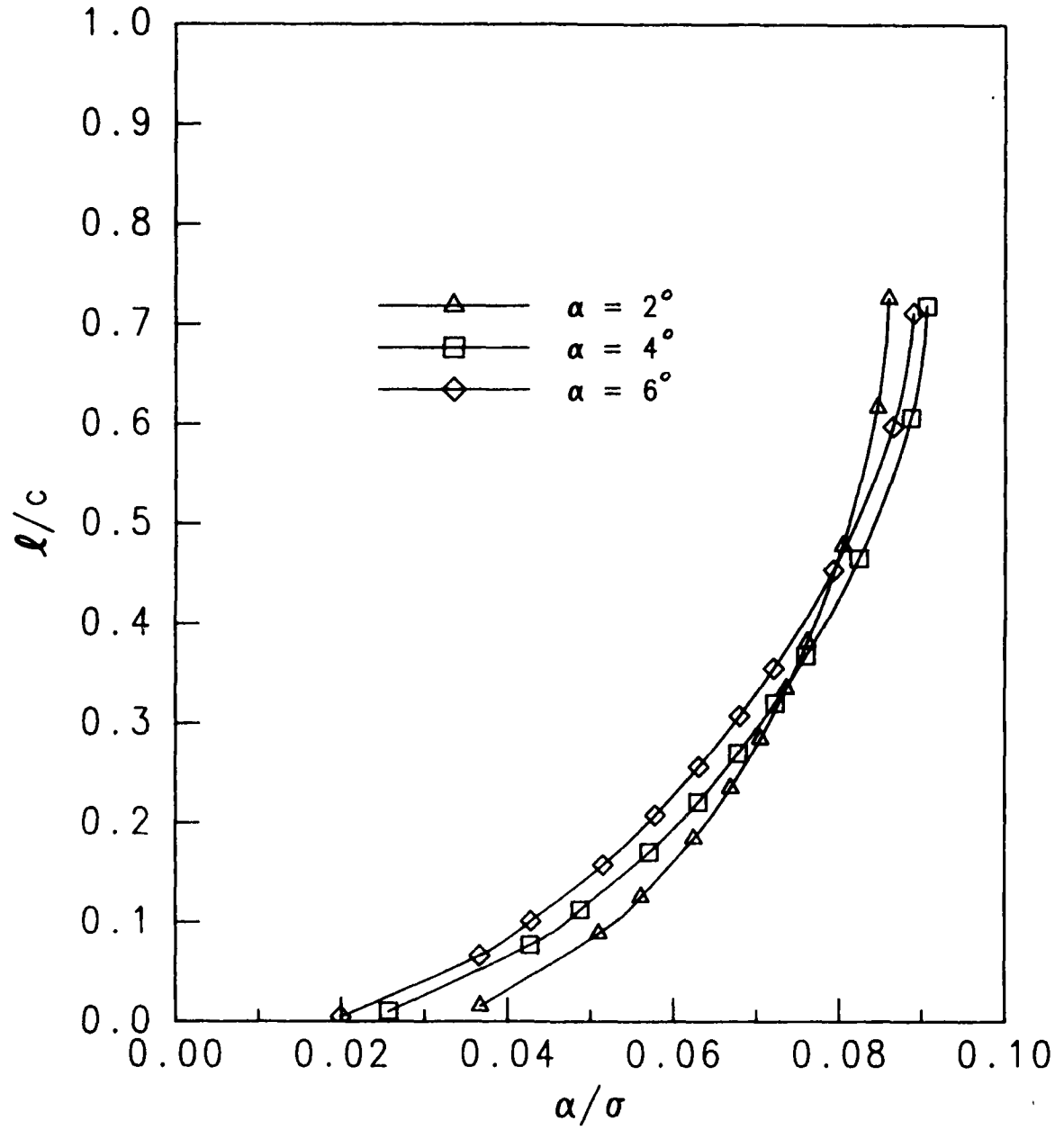

Figure 3 - Effect of Angle of Attack on Cavity Length for NACA 66-006 Section

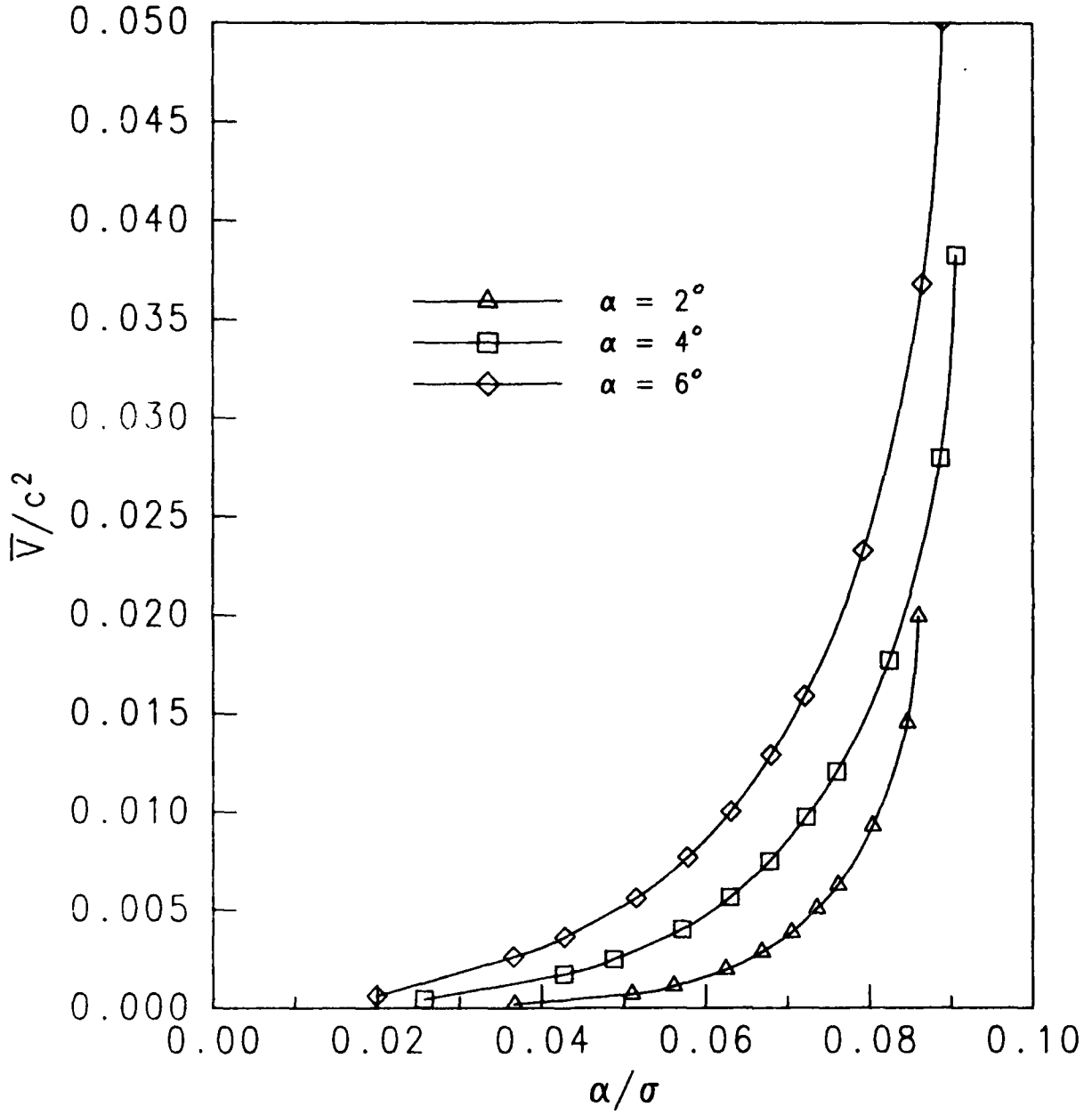

Figure 4 - Effect of Angle of Attack on Cavity Volume for NACA 66-006 Section

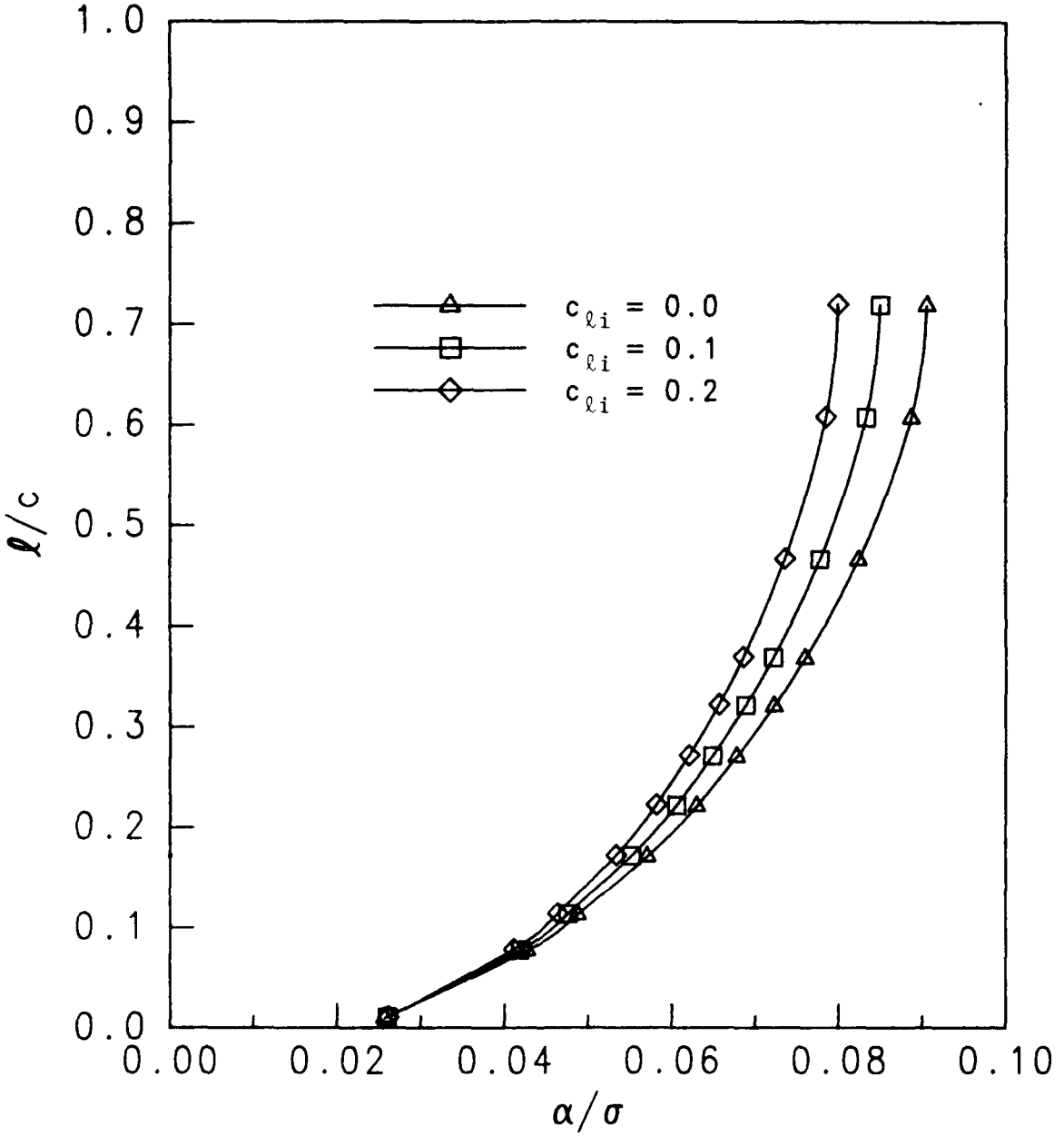

Figure 5 - Effect of Camber on Cavity Length for NACA 66-006 Section

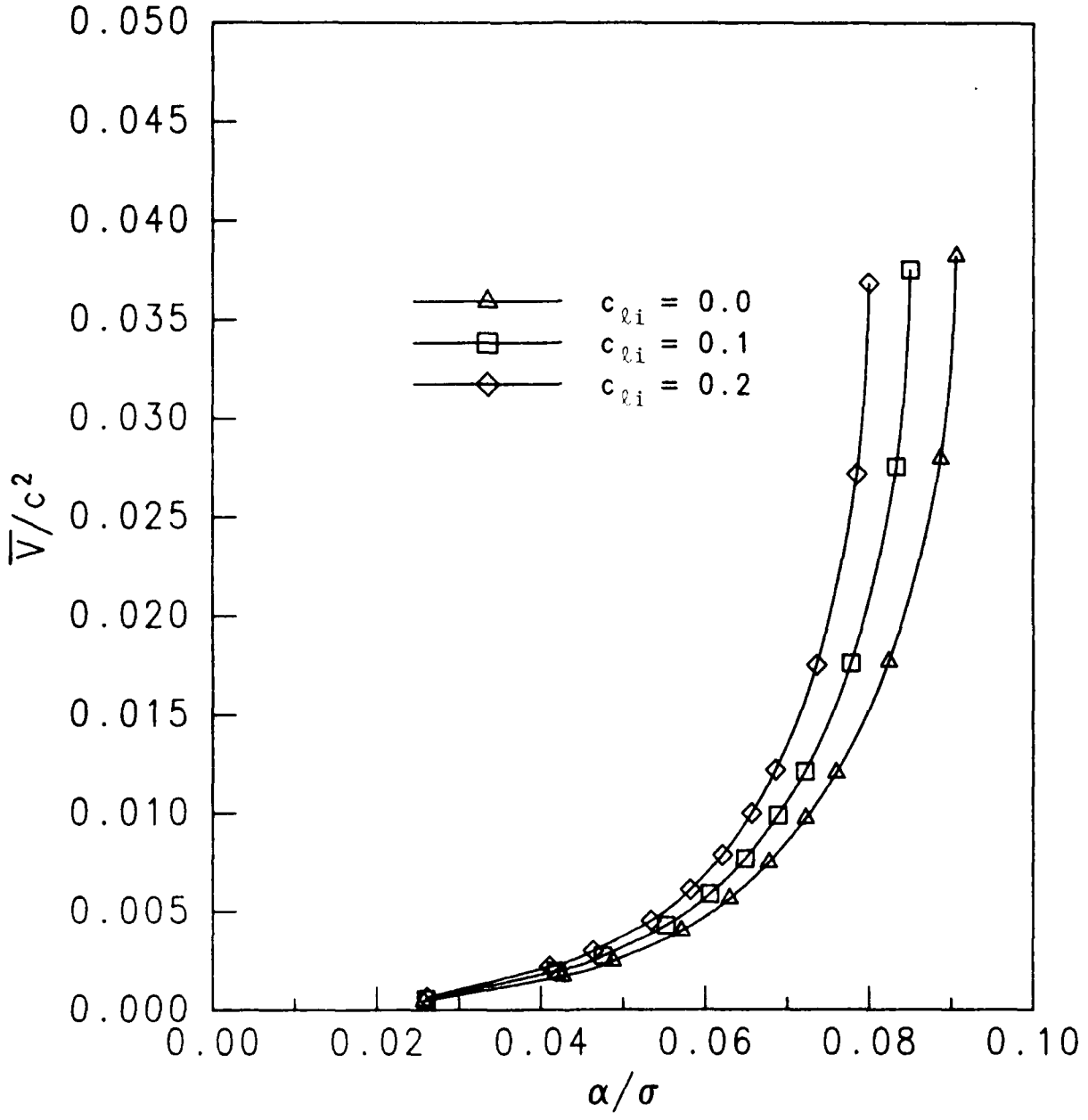

Figure 6 - Effect of Camber on Cavity Volume for NACA 66-006 Section

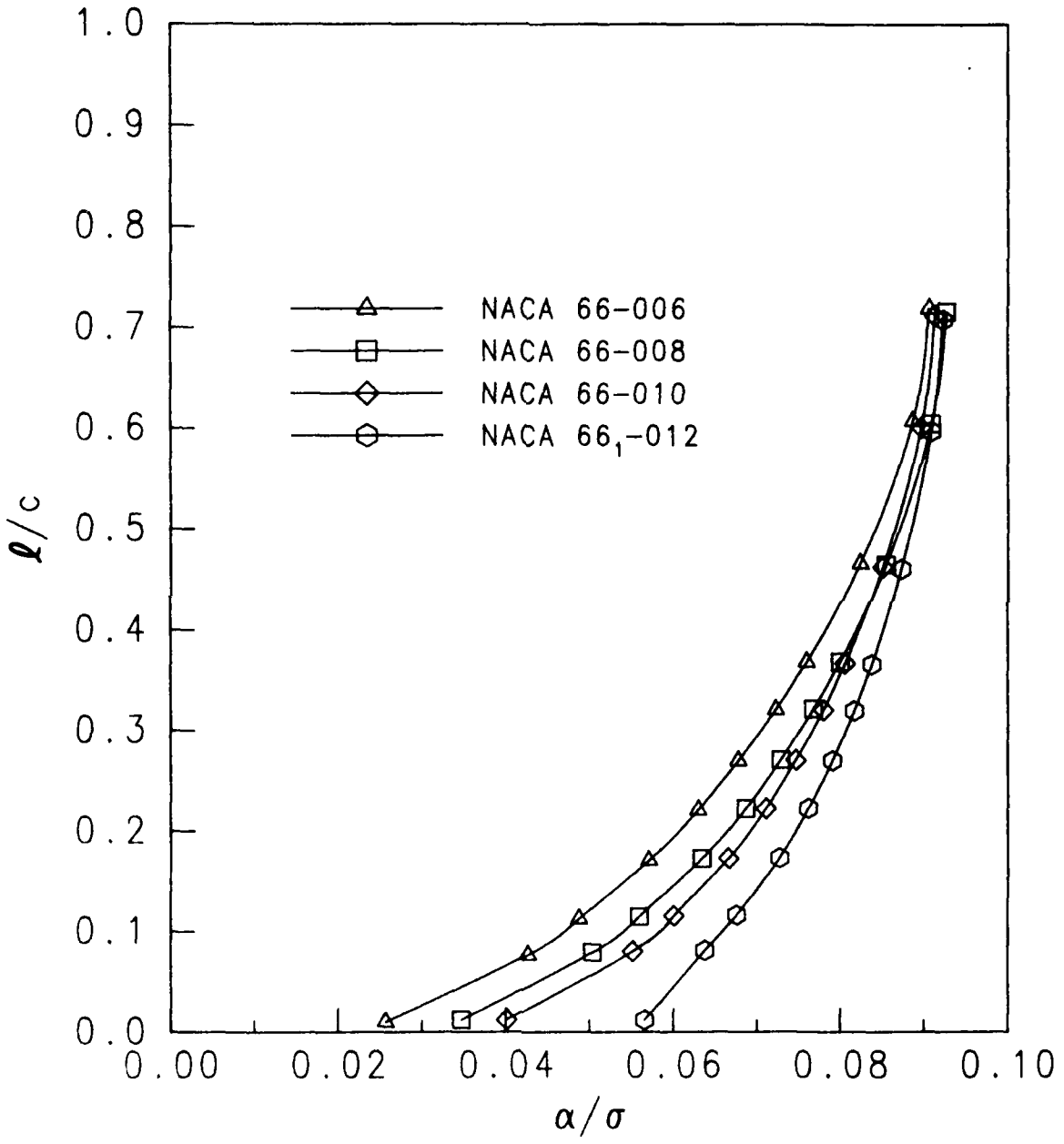

Figure 7 - Effect of Thickness on Cavity Length for Series NACA 66 Sections, $\gamma = 4°$

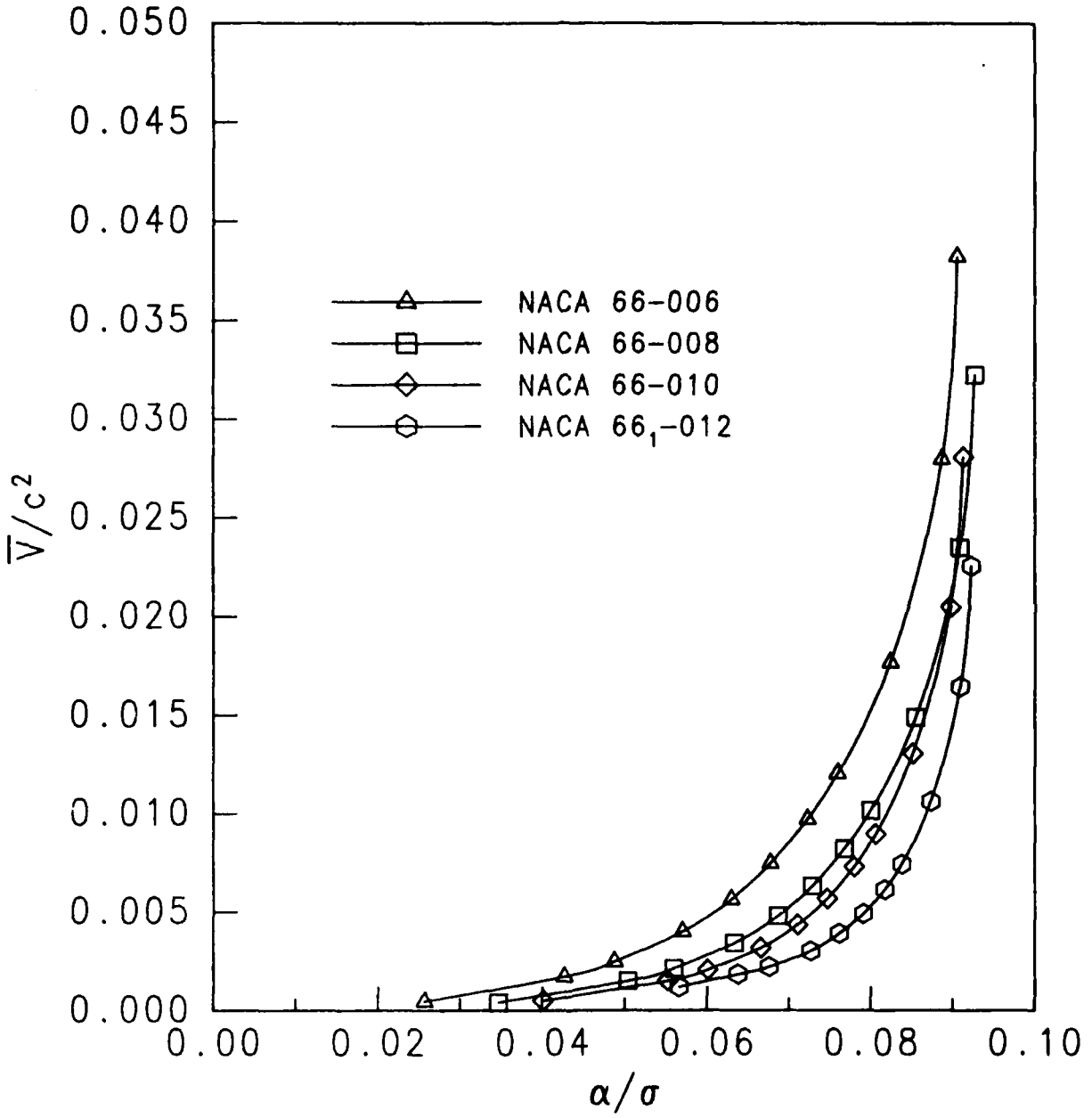

Figure 8 - Effect of Thickness on Cavity Volume for Series NACA 66 Sections, $\alpha = 4°$

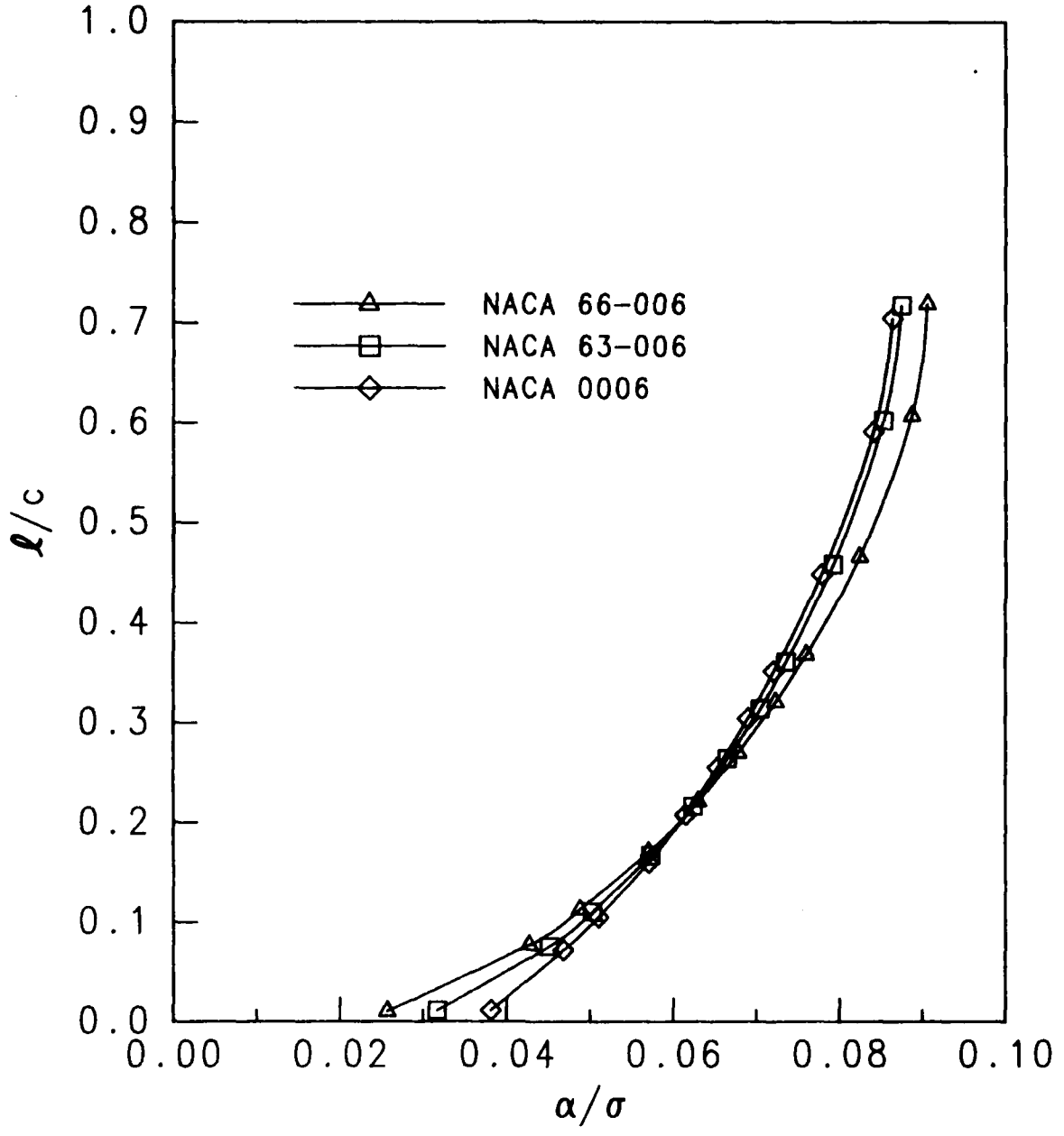

Figure 9 - Effect of Thickness Distribution on Cavity Length, $\alpha = 4°$

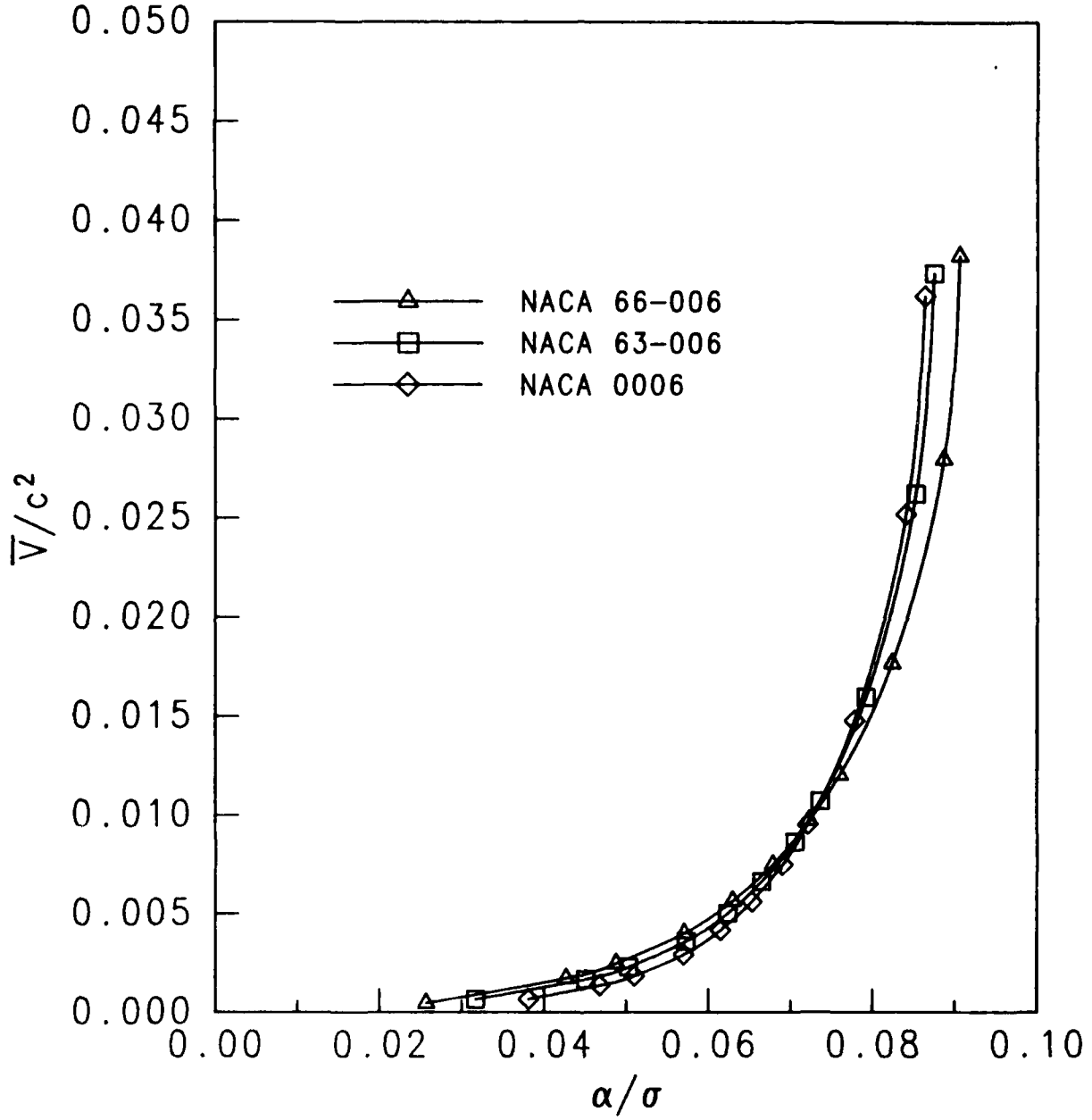

Figure 10 - Effect of Thickness Distribution on Cavity Volume, α = 4°

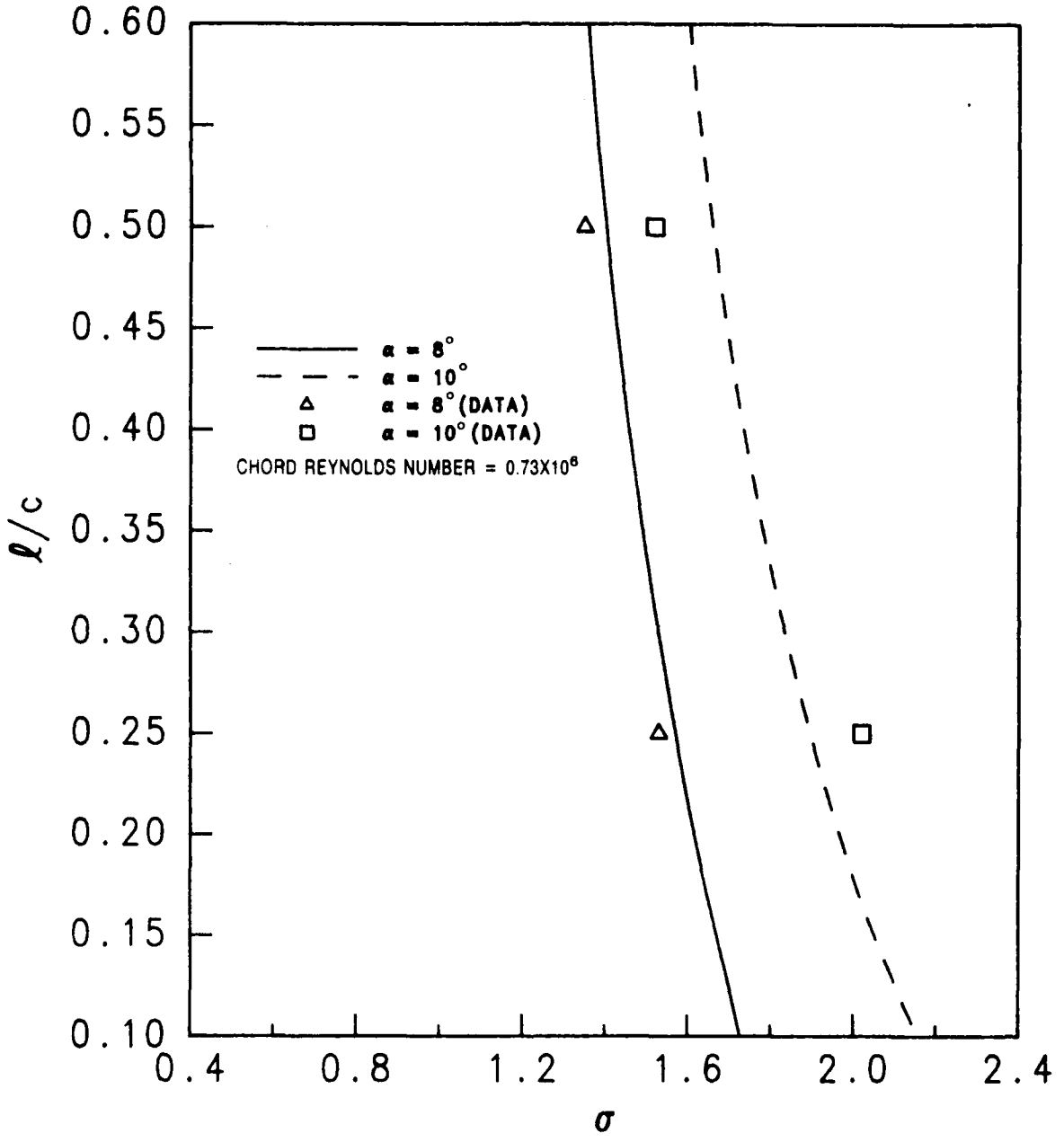

Figure 11 - Comparison with Experimental Data of Kermeen for NACA 4412 Section

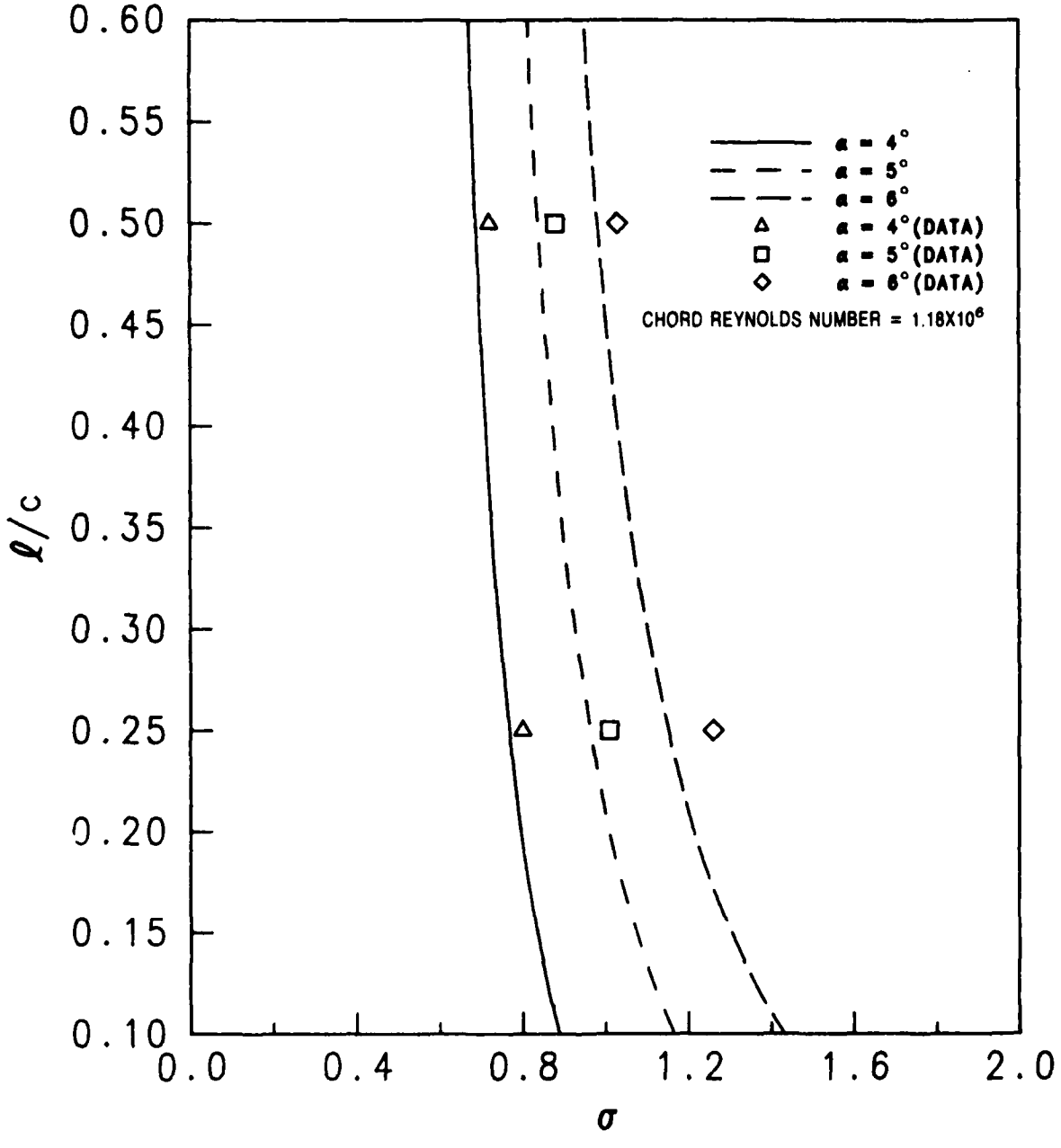

Figure 12 - Comparison with Experimental Data of Kermeen for NACA 66_1-012 Section

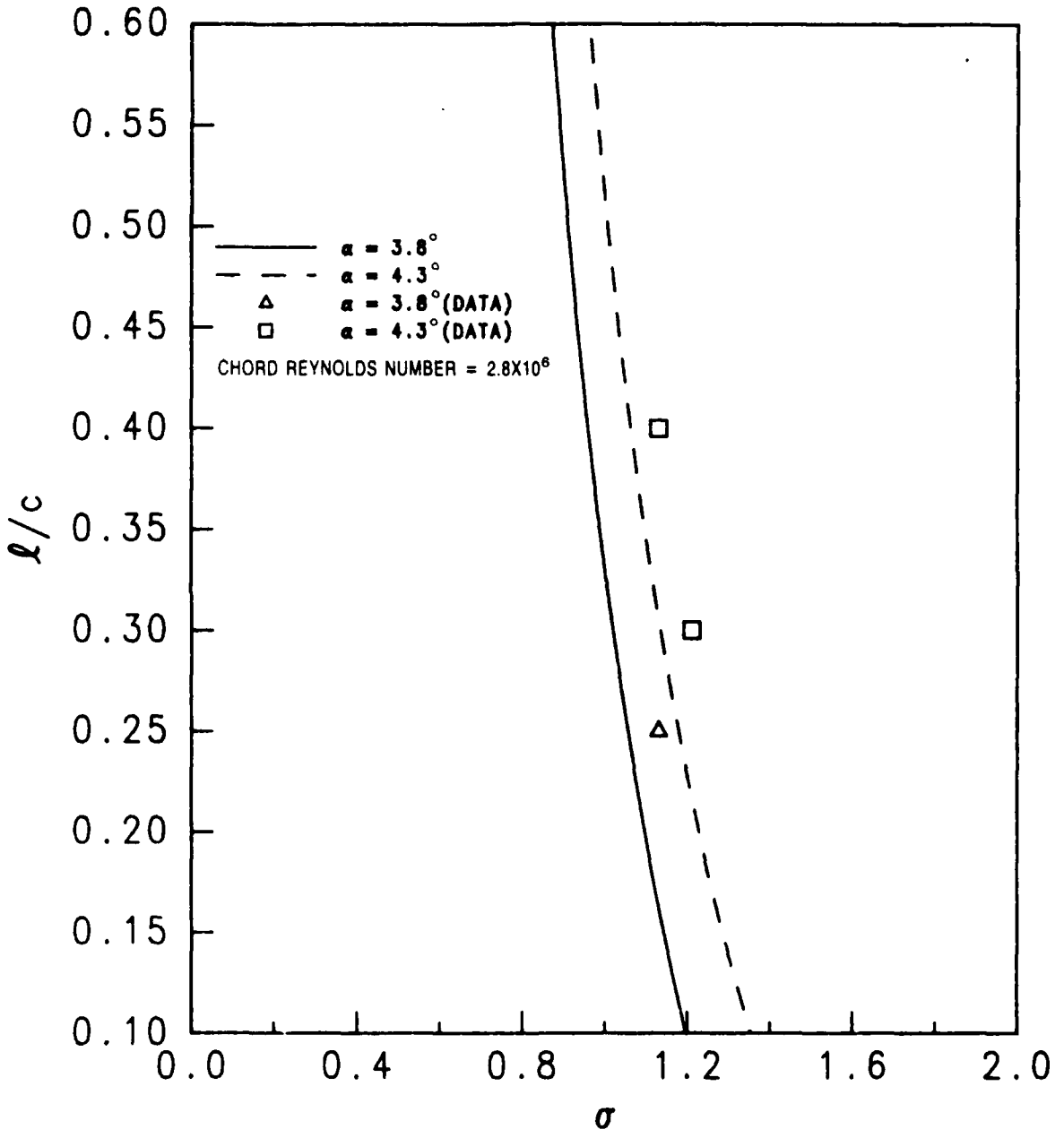

Figure 13 - Comparison with Experimental Data of Shen and Peterson for 10.5% Joukowsky Section

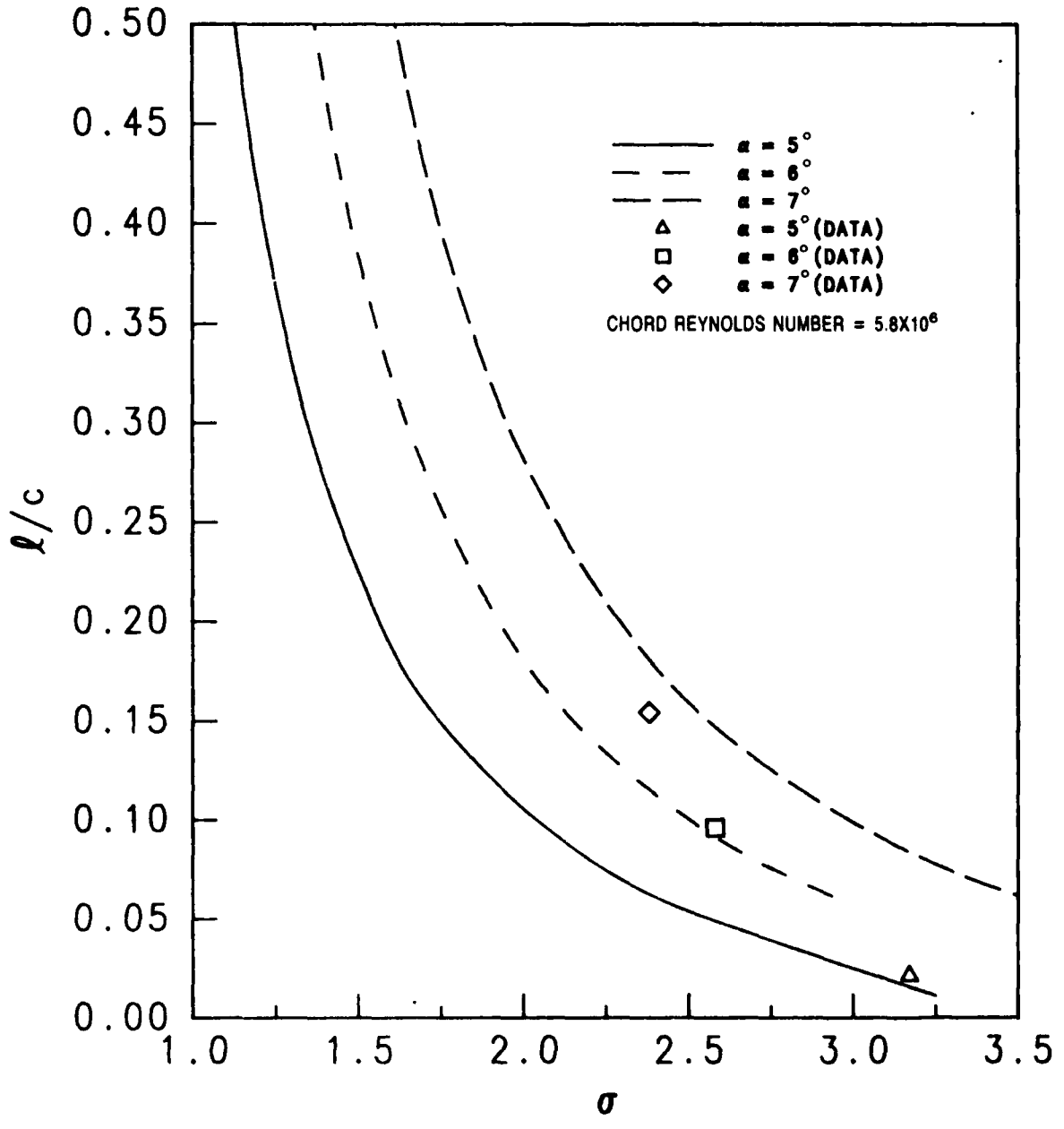

Figure 14 - Comparison with Experimental Data of McCullough and Gault for NACA 64A006 Section

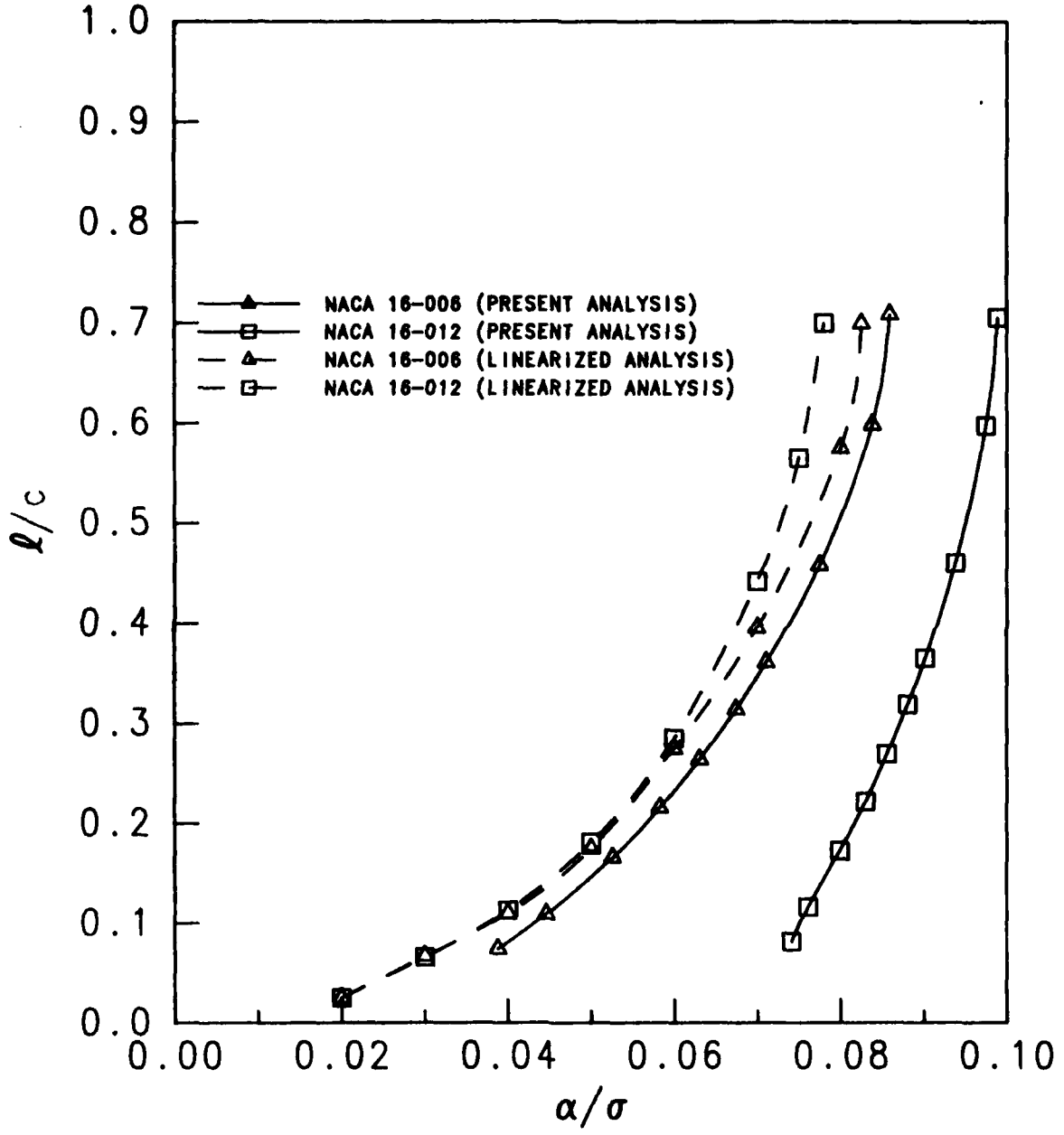

Figure 15 - Comparison with Linear Numerical Analysis for NACA 16 Sections, $\alpha = 4°$

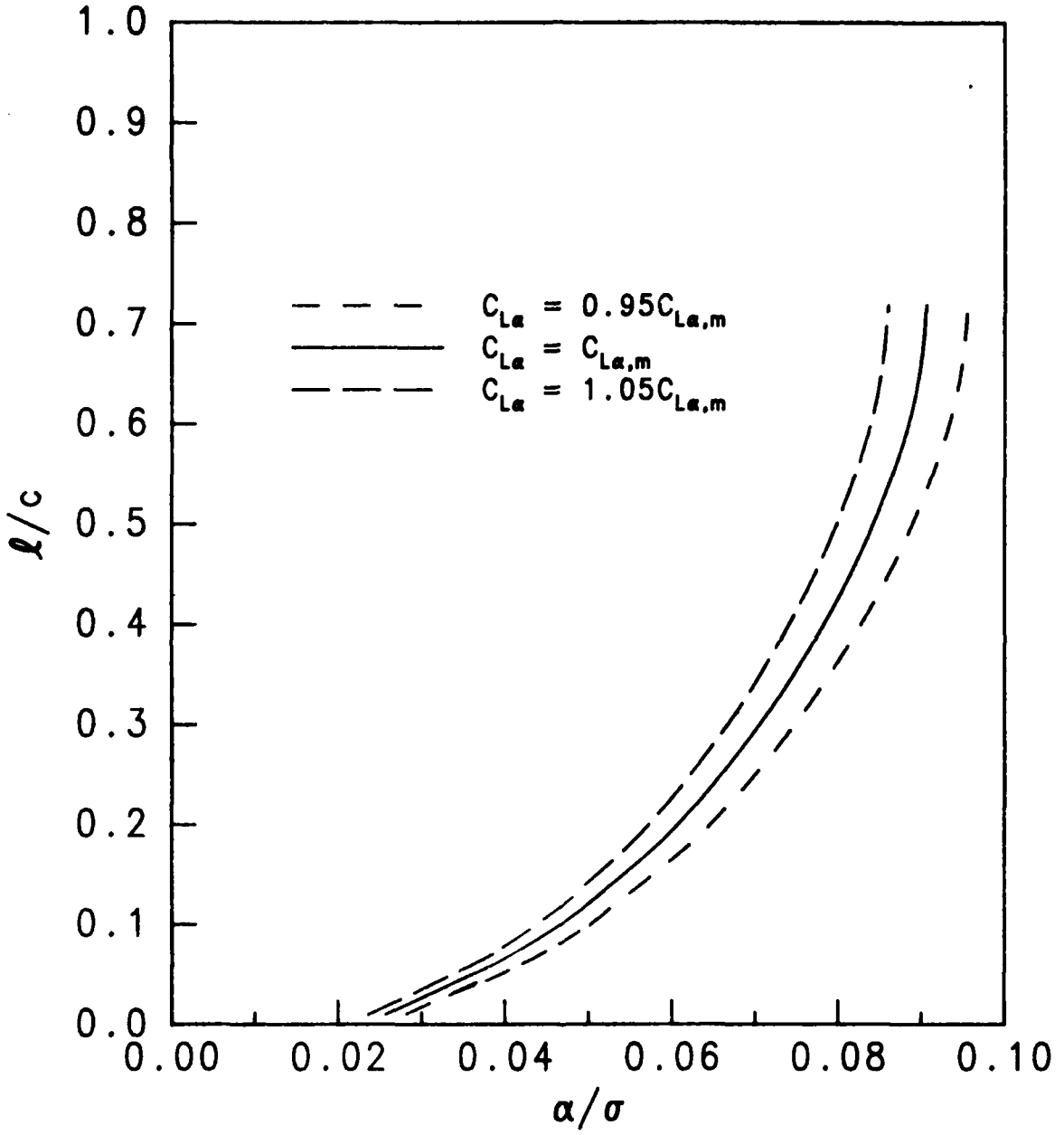

Figure 16 - Effect of Fully Wetted Flow Lift Curve Slope on Cavity Length for NACA 66-006 Section, $\alpha = 4°$

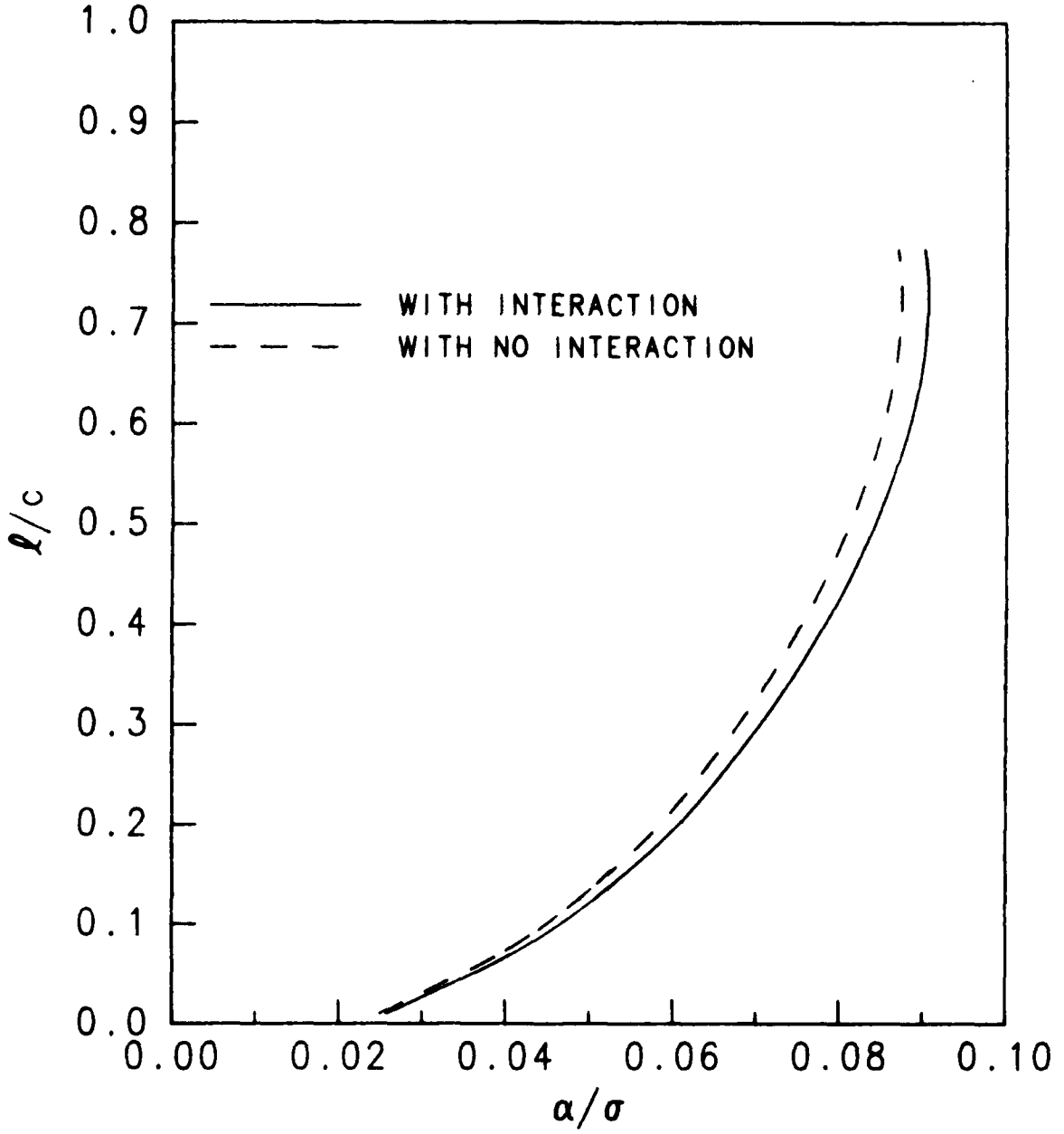

Figure 17 - Interaction Effect of Fully Wetted and Cavitating Flows on Cavity Length for NACA 66-006 Section, $\tau = 4°$

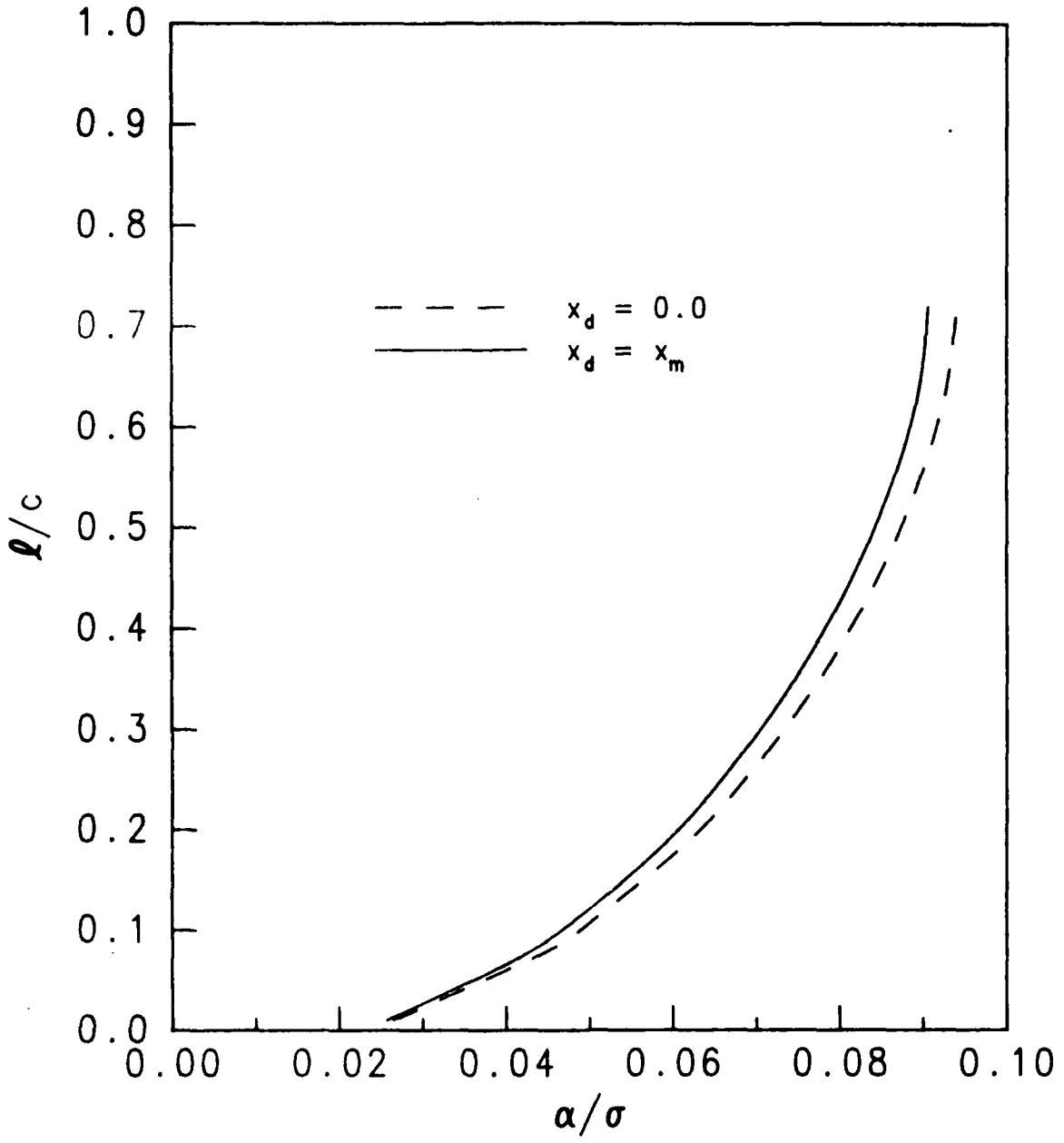

Figure 18 - Effect of Cavity Detachment Position on Cavity Length for NACA 66-006 Section, $\alpha = 4°$

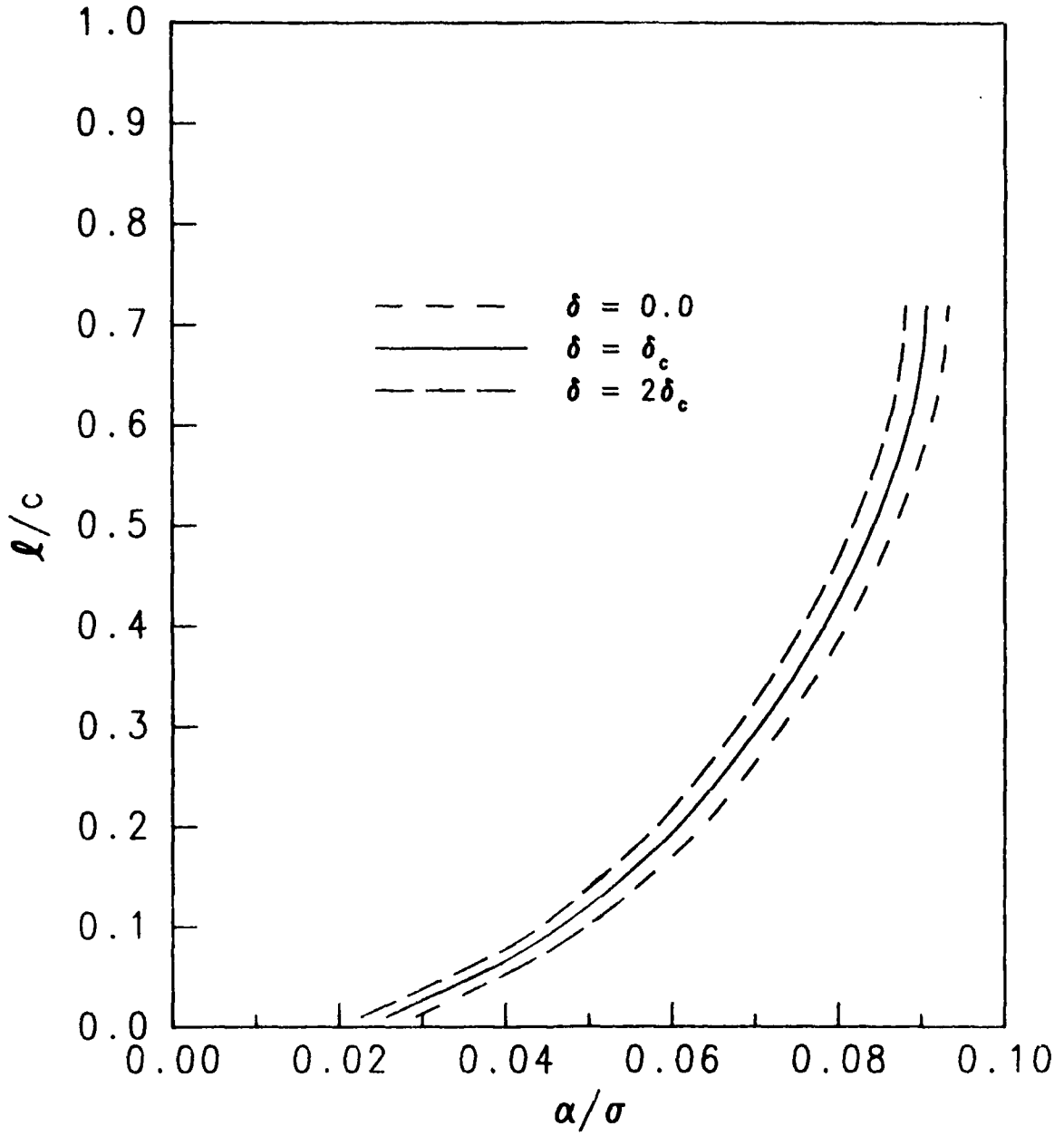

Figure 19 - Effect of Cavity Closure Condition on Cavity Length for NACA 66-006 Section, $\alpha = 4°$

INITIAL DISTRIBUTION

Copies	
1	ARMY CHIEF OF RES & DIV
1	ARMY ENGR R&D LAB
3	CHONR
	1 Code 438
	1 Lib
	1 Lee
4	ONR BOSTON
4	ONR CHICAGO
4	ONR LONDON, ENGLAND
1	NRL
2	USNA
	1 Lib
	1 Johnson
1	NAVPGSCOL Lib
1	NROTC & NAVADMINU, MIT
1	NADC
5	NOSC
	1 1311 Lib
	1 6005
	1 13111 Lib
	1 2501/Hoyt
	1 Nelson
1	NWC
37	NAVSEA
	3 SEA 05H
	5 SEA 05R
	1 SEA 55
	1 SEA 55D
	1 SEA 55N
	3 SEA 55W
	1 SEA 56D
	1 SEA 56X
	3 SEA 56X1
	1 SEA 56X2

Copies	
	NAVSEA (Continued)
	1 SEA 56X4
	1 SEA 56X5
	1 SEA 56XP
	1 PMS-378
	1 PMS-380
	1 PMS-381
	1 PMS-383
	1 PMS-389
	1 PMS-391
	1 PMS-392
	1 PMS-393
	1 PMS-393
	1 PMS-397
	1 PMS-399
	1 PMS-400
	1 SEA Tech Rep Bath, England
	2 DET NORFOLD (Sec 6660)
2	MMA
	1 Lib
	1 Maritime Res Cen
1	FAC 032C
1	MILITARY SEALIFT COMMAND (M-4EX)
1	NAVSHIPYD/PTSMH
1	NAVSHIPYD/PHILA
1	NAVSHIPYD/NORVA
1	NAVSHIPYD/CHASN
1	NAVSHIPYD/LBEACH
1	NAVSHIPYD/MARE
1	NAVSHIPYD/PUGET
1	NAVSHIPYD/PEARL
12	DTIC
2	HQS COGARD

Copies	
1	US COAST GUARD (G-ENE-4A)
1	LC/SCI & TECH DIV
7	MARAD 1 DIV SHIP DES 1 COORD RES 1 Shubert 1 Dashnaw 1 Hammer 1 Lasky 1 Siebold
2	NASA STIF 1 DIR RES
1	NSF ENGR DIV Lib
1	DOT Lib
1	U BRIDGEPORT/URAM
2	U CAL BERKELEY/DEPT NAME 1 NAME Lib 1 Webster
1	U CAL SAN DIEGO/Ellis
2	UC SCRIPPS 1 Pollack 1 Silverman
1	U MARYLAND/GLENN MARTIN INST
1	U MISSISSIPPI/DEPT OF M.E.
4	CIT 1 AERO Lib 1 Acosta 1 Plesset 1 Wu
1	CATHOLIC U
1	COLORADO STATE U/Albertson
1	U CONNECTICUT/Scottron

Copies	
1	CORNELL U/Sears
1	FLORIDA ATLANTIC U OE Lib
3	HARVARD U 1 McKay Lib 1 Birkoff 1 Carrier
2	U HAWAII/Bretschneider
1	U ILLINOIS/Robertson
3	U IOWA 1 IHR/Kennedy 1 IHR/Landweber 1 IHR/Stern
2	Johns Hopkins U 1 Phillips 1 Inst Coop Res
1	U KANSAS CIV ENGR Lib
1	KANSAS ST U ENGR EXP/Lib
1	LEHIGH U FRITZ ENGR LAB Lib
1	LONG ISLAND U
3	U MICHIGAN/DEPT NAME 1 NAME Lib 1 Parsons 1 Vorus
5	MIT 1 BARKER ENGR Lib 2 OCEAN ENGR/Kerwin 1 OCEAN ENGR/Leehey 1 OCEAN ENGR/Newman
3	U MINNESOTA SAFHL 1 Killen 1 Song 1 Wetzel

Copies	
2	STATE U MARITIME COLL S U ARL Lib 1 ENGR DEPT 1 INST MATH SCI
1	NOTRE DAME ENGR Lib
5	PENN STATE U ARL 1 Lib 1 Henderson 1 Gearhart 1 Parkin 1 Thompson
1	PRINCETON U/Mellor
1	RENSSELAER/DEPT MATH
1	ST JOHNS U
1	VIRGINIA TECH/KAPLAN
3	SWRI 1 APPLIED MECH REVIEW 1 Abramson 1 Burnside
1	BOEING ADV AMR SYS DIV
3	BOLT BERANEK AND NEWMAN 1 Brown 1 Jackson 1 Greeley
1	BREWER ENGR LAB
1	CAMBRIDGE ACOUS/Junder
1	CALSPAN, INC/Ritter
1	STANDFORD U/Ashley
1	STANDFORD RES INST Lib
3	SIT DAVIDSON LAB 1 Lib 1 Breslin 1 Tsakonas

Copies	
1	TEXAS U ARL Lib
1	UTAH STATE U/Jeppson
2	WEBB INST 1 Ward 1 Hadler
1	WHOI OCEAN ENGR DEPT
1	WPI ALDEN HYDR LAB Lib
1	ASME/RES COMM INFO
1	ASNE
1	SNAME
1	AERO JET-GENERAL/Beckwith
1	ALLIS CHALMERS, YORK, PA
1	AVCO LYCOMING
1	BAKER MANUFACTURING
2	BATH IRON WORKS CORP 1 Hansen 1 FFG7 PROJECT OFFICE
1	BETHLEHEM STEEL SPARROWS POINT
3	BIRD-JOHNSON CO 1 Case 1 Ridley 1 Norton
2	DOUGLAS AIRCRAFT 1 TECHNICAL Lib 1 Smith
1	EXXON RES DIV/Lib
1	FRIEDE & GOLDMAN/Michel

Copies	
2	GEN DYN CONVAIR ASW-MARINE SCIENCES
3	GIBBS & COX 1 TECH Lib 1 Olson 1 CAPT Nelson
1	GRUMMAN AEROSPACE/Carl
1	TRACOR/HYDRONAUTICS/Lib
1	INGALLS SHIPBUILDING
1	INST FOR DEFENSE ANAL
1	ITEK VIDYA
1	LIPS DURAN/Kress
1	LITTLETON R & ENG CORP/Reed
1	LITTON INDUSTRIES
1	LOCKHEED/Waid
1	MARITECH, INC/Vassilopoulis
1	HYDRODYNAMICS RESEARCH ASSOCIATES, INC/Cox
1	NATIONAL STEEL & SHIPBUILDING
1	NEWPORT NEWS SHIPBUILDING Lib
1	NIELSEN ENGR/Spangler
1	NKF Associates/Noonan
1	NAR SPACE/Ujihara
2	ORI, INC 1 Bullock 1 Amato

Copies	
1	PROPULSION DYNAMICS, INC
1	PROPULSION SYSTEMS, INC
1	SCIENCE APPLICATIONS INTERNATIONAL CORP/Salvesen
1	GEORGE G. SHARP
1	SPERRY SYS MGMT Lib/Shapior
1	SUN SHIPBLDG/Lib
2	TETRA TECH PASADENA 1 Chapkis 1 Furuya
1	UA HAMILTON STANDARD/Cornell

CENTER DISTRIBUTION

Copies	Code	Name
1	0120	
1	11	
1	1102.1	Nakonechny
1	15	W.B. Morgan
1	1504	V. J. Monacella
1	1506	Hawkins
1	1508	Boswell
1	1509	Powell
1	152	Lin
1	1521	Day
1	1521	Karafiath
1	1521	Hurwitz
1	1522	Dobay
1	1522	Remmers
1	1522	Wilson
20	1522	Hsu

CENTER DISTRIBUTION

Copies	Code	Name
1	154	McCarthy
1	1542	Huang
1	1542	Shen
1	1543	Jeffers
1	1543	Wisler
1	1544	Caster
1	1544	Reed
1	1544	Fuhs
1	1544	Jessup
1	1544	Kim
1	1544	Lin
1	156	Cieslowski
1	1561	Feldman
1	1561	O'Dea
1	1562	Moran
1	1563	Milne
1	1564	Cox
1	172	Krenzke
1	1720.6	Rockwell
1	19	Sevik
1	19	Strasberg
1	1903	Chertock
1	1905	Blake
1	1942	Archibald
1	1942	Mathews
1	1962	Zaloumis
1	1962	Noonan
1	1962	Kilcullen
1	2814	Czyryca
10	5211.1	Reports Distribution
1	522.1	TIC (C)
1	522.2	TIC (A)

END

DTIC

7-86